CP-225,917 and CP-263,114: Novel Ras Farnesylation Inhibitors from an Unidentified Fungus. 2. Structure Elucidation

Thomas T. Dabrah, Takushi Kaneko,* Walter Massefski, Jr., and Earl B. Whipple

Contribution from Pfizer Central Research, Groton, Connecticut 06340

Received March 26, 1996[⊗]

Abstract: The structure elucidations of new fungal products CP-225,917 and CP-263,114 are described. The structures, including relative stereochemistry, were established using a variety of analytical data and extensive NMR analysis. The compounds possess a bicyclo[4.3.1]deca-1,6-dien-10-one system in conjunction with a maleic anhydride moiety, a γ-lactol, and two alkenyl side chains. They are related to nonadrides, and their biosynthetic origins are proposed. The producing organism also yields zaragozic acid A, and both zaragozic acids and compounds CP-225,917 and CP-263,114 appear to be derived from the condensation of oxaloacetic acid and the corresponding monocarboxylic acid.

Introduction

There is substantial interest in discovering an inhibitor of squalene synthase (SQS), since this enzyme represents the first committed step of cholesterol biosynthesis starting from farnesyl pyrophosphate (FPP).[1] Such an inhibitor can be used to control the level of serum cholesterol without affecting the production of nonsterol compounds derived from FPP.[1,2]

Ras farnesyl transferase is another enzyme which utilizes FPP as a substrate.[3,4] Farnesylation of ras protein is a necessary step for its membrane localization where it functions as a molecular switch for cell growth. Inhibition of ras farnesylation is thus considered an effective approach to control abnormal growth of cells transformed by mutated ras.[5,6]

While screening for novel inhibitors of squalene synthase and protein farnesyl transferase, we discovered CP-225,917 (**1**) and CP-263,114 (**2**) in the culture broth of an unidentified fungus. Compounds **1** and **2** inhibit ras farnesyl transferase from rat brain with IC$_{50}$ values of 6 and 20 μM, respectively. The former compound also inhibits squalene synthase isolated from rat liver microsomes with an IC$_{50}$ value of 43 μM while the latter compound does so with an IC$_{50}$ of 160μM.[7] Their structures indicate an unusual arrangement of functional groups including a bicyclo[4.3.1]deca-1,6-diene system, a bridgehead double bond, a lactol or lactol acetal system, and a maleic anhydride moiety. The structure elucidation of these compounds is based mainly on extensive NMR measurements and will be described in this paper. Their biosynthetic relationship to some natural products will also be discussed.

Results and Discussion

The producing organism was isolated from a juniper twig in Texas and appears to have characteristics of a sterile *Phoma* species. From 15 L of the fermentation broth, approximately 31 mg of CP-225,917 (**1**), 18 mg of CP-263,114 (**2**), and 8 mg

of zaragozic acid A (squalestatin I)[8,9] were isolated by reverse phase HPLC.

The molecular weight of CP-225,917 (**1**) was determined to be 570 by both positive FAB-MS [571 (M + H)] and negative FAB-MS [569 (M − H)]. This was further confirmed by addition of sodium iodide where the M + Na peak (593) was also observed. The high-resolution FAB-MS indicated a molecular formula of C$_{31}$H$_{38}$O$_{10}$ (calcd for M + H 571.2542, found 571.2532). In a similar fashion, the molecular weight of CP-263,114 (**2**) was determined to be 552, and its molecular formula was determined to be C$_{31}$H$_{36}$O$_9$ (calcd for M + H 553.2437, found 553.2427). Compound **1** had [α]$^{25}_D$ of +23° (*c* 0.5, CH$_2$Cl$_2$), whereas compound **2** had [α]$^{25}_D$ of −11° (*c* 0.5, CH$_2$Cl$_2$). The UV spectra showed absorption at 250 nm for both compounds, suggesting an α,β-unsaturated carbonyl group. The FT-IR spectra exhibited bands which implied the presence of a carboxylic acid (3500−3200, 1710 cm^{-1}), an anhydride (1830, 1760 cm^{-1}), and a long-chain methylene moiety(ies) (720 cm^{-1}).

The ^{1}H NMR and ^{13}C NMR spectra of **1** and **2** are similar, and this points to a close structural homology between these compounds. The ^{13}C NMR spectra in chloroform-*d* solution were complicated by nonuniform intensities and line widths, which were traced to large (>10-fold) variations in spin-lattice relaxation time. The nT_1 measurements for the methine and methylene groups were consistent with a general model for a structure consisting of two mobile side chains attached to a rigid cage (these variations in T_1 were useful in concomitantly tracing sequential connections through overlapping regions of the COSY spectra). The ^{13}C relaxation times imply that the correlation times in the cage are near the T_1 minimum, consistent with the fact that NOEs between protons on the cage are negative (slow motion limit) in compound **1** and almost vanish in compound **2**.

⊗ Abstract published in *Advance ACS Abstracts,* February 1, 1997.
(1) Poulter, C. D. *Acc. Chem. Res.* **1990,** *23,* 70−77.
(2) Goldstein, J. L.; Brown, M. S. *Nature* **1990,** *343.*
(3) Maltese, W. A. *FASEB J.* **1990,** *4,* 3319−3328.
(4) Clarke, S. *Annu. Rev. Biochem.* **1992,** *61,* 355−386.
(5) Gibbs, J. B. *Cell* **1991,** *65,* 1−4.
(6) Hancock, J. F. *Curr. Biol.* **1993,** *3,* 770−772.
(7) Dabrah, T. T.; Harwood, H. J.; Huang, L. H.; Jankovich, N. D.; Kaneko, T.; Li, J.-C.; Lindsey, S.; Moshier, P. M.; Subashi, T. A.; Therrien, M.; Watts, P. C. *J. Antibiot.* **1997,** *50,* 1−7.

(8) Dawson, M. J.; Farthing, J. E.; Marshall, P. S.; Middleton, R. F.; O'Neill, M. J.; Shuttleworth, A.; Stylli, C.; Tait, R. M.; Taylor, P. M.; Wildman, H. G.; Buss, A. D.; Langley, D.; Hayes, M. V. *J. Antibiot.* **1992,** *45,* 639−647.
(9) Bergstrom, J. D.; Kurtz, M. M.; Rew, D. J.; Amend, A. M.; Karkas, J. D.; Bostedor, R. G.; Bansol, V. S.; Dufrensne, C.; Van Middleworth, F. L.; Hensens, O. D.; Liesch, J. M.; Zink, D. L.; Wilson, K. E.; Onishi, J.; Milligan, J. A.; Bills, G.; Kaplan, L.; Nallin-Omstead, M.; Jenkins, R. G.; Huang, L.; Meinz, M. S.; Quinn, L.; Burg, R. W.; Kong, Y.; Mochales, S.; Mojena, M.; Martin, M.; Peláez, F.; Diez, M. T.; Alberts, A. W. *Proc. Nat. Acad. Sci. U.S.A.* **1993,** *90,* 80−84.

Table 1. ^{1}H and ^{13}C NMR Data for **1** and **2** in CDCl$_3$

position	^{13}C shift	H no.	H shift	^{13}C nT_1	^{1}H–^{1}H correlations	LRCOSY	HMBC	position	^{13}C shift	H no.	H shift	^{13}C nT_1	^{1}H–^{1}H correlations	LRCOSY	HMBC
				Compound **1**								Compound **2**			
1	17.9	3	1.66		H2	H3		1	17.9	3	1.64				
2	129.1	1	5.43	>2	1	4		2	129.3	1	5.40				
3	126.4	1	5.52	>3	4	1		3	126.2	1	5.48				
4	26.4	2	2.34	1.40	3,5	2		4	26.0	2	2.28	1.63	H5		
5	38.2	2	2.69	0.88	4			5	38.3	2	2.66	1.17	4		C6
6	211.7	0					H4,5,7	6	207.6	0					
7	76.0	1	4.59	0.37	8			7	75.1	1	4.56	0.40	8		6
8	39.3	2	2.19	0.26	7,9			8	35.2	2	2.58	0.43	7,9		
			1.97								2.06				6,7
9	43.5	1	1.53	0.27	8,17			9	35.4	1	2.34	0.35	8,10		7,26
10	47.6	1	4.11	0.32		13		10	43.2	1	3.53	0.38	9	H13	11,12,15,26,31
11	144.7	0					9,10,13	11	141.5	0					
12	137.7	0					10,13	12	140.3	0					
13	39.4	2	2.98	0.32		10		13	40.2	2	3.06	0.46		10	11,12,14,15
			2.56								2.71			10	11,12,14,27,30
14	48.4	0					13,16,28	14	47.3	0					
15	141.1	0					10,28	15	139.8	0					
16	129.3	1	5.82	0.37		17		16	129.3	1	5.65			17	9,14,26
17	40.4	1	2.41	0.27	9,18	16		17	43.2	1	2.30	0.39		16	
18	34.1	2	1.61	0.32	17,19		16	18	36.1	2	1.27	0.49			
			1.23								1.27				
19	27.6	2	1.45	0.49	18			19	26.8	2	1.20	0.70			
			1.29								1.20				
20	29.1	2	1.38	0.76				20	28.9	2	1.25	1.09			
			1.27								1.25				
21	29.4	2	1.35	1.17	22			21	29.2	2	1.30	1.68			
22	32.5	2	1.97	1.44	21,23	24		22	32.3	2	1.96	2.02			
23	124.9	1	5.42	>3	22	25		23	125.0	1	5.41				
24	131.2	1	5.42	>2.5	25	22		24	131.0	1	5.38				
25	17.9	3	1.66		24	23			18.0	3	1.64				
26	105.4	0					9,10,16	26	104.8	0					
27	176.1	0					13	27	175.3	0					
28	36.9	2	3.26	0.32				28	37.3	2	3.29	0.39			14,15,29
			2.99								2.95				14,27,29
29	173.1	0					28	29	173.8	0					
30	164.9	0						30	164.3	0					
31	165.5	0					10	31	164.4	0					

The multiplicity-edited ^{13}C NMR spectrum (DEPT) revealed the presence of 2 CH$_3$-, 10 CH$_2$-, 9 CH-, and 10 quarternary carbons for both **1** and **2**. The molecular formula for compound **1** shows three additional hydrogens and therefore suggested three exchangeable hydroxyl groups (these molecules have no nitrogen or sulfur). By similar analysis, compound **2** has a single hydroxyl. The nature and location of the three hydroxyl groups in **1** were determined by means of ^{13}C isotope shifts on ^{2}H exchange. Two carbon signals at 76.0 and 105.4 ppm were split by −0.1 ppm on addition of HDO, showing attached hydroxyls undergoing slow chemical exchange, while the carbon signal at 173.8 ppm showed an averaged shift (confirmed by successive washes with D$_2$O and H$_2$O) indicative of a carboxyl group undergoing rapid exchange. Inspection of the ^{13}C chemical shifts showed that there is a single ketone (211.7 ppm), four ester or acid carbonyls (in the range 160−180 ppm), a single alkoxy carbon (76.0 ppm), and another oxygenated carbon (105.4 ppm). There are eight vinyl carbons (between 124 and 145 ppm) in each molecule; thus, the molecular formula predicts four rings for **1**. From a similar analysis, five rings are predicted for **2**.

Experiments have shown that compound **1** is converted to **2** upon treatment with a catalytic amount of methanesulfonic acid, while the reverse does not occur. Therefore, the simplest way to incorporate the chemical interconversion with the disappearance of two hydroxyls and the gain of a ring in going from **1** to **2** is to infer that the hydroxy and hemiacetal fuse to form an internal acetal. This in turn suggested that a proposal for one structure could lead to the structure of the other.
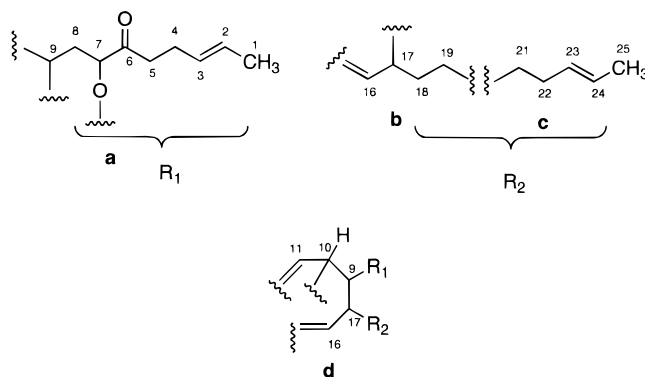
Figure 1. Units from ^{1}H–^{1}H COSY and ^{1}H–^{13}C HMBC experiments.

NMR Structure Connectivities. The construction of the molecular framework was based on a combination of COSY (including long-range COSY) and HMBC experiments (Table 1). In compound **1**, three major spin systems were observed, comprising carbons 1−9 (see **a** in Figure 1), carbons 16−19, and carbons 21−25 (see **b** and **c** in Figure 1). In addition, a COSY connection was observed between H-9 and H-17, and HMBC correlations between H-9 and C-11 and H-10 and C-11 allowed the methine unit at C-10 to be positioned as shown (**d**). HMBC data of **2** were used to place a keto carbonyl group into R$_1$ adjacent to the carbon atom bearing an alkoxy group. The side chains contain four of the eight vinyl units, allowing the remainder to be combined into the cage structure (see below). The magnitude of their vinylic proton coupling (≥ 14
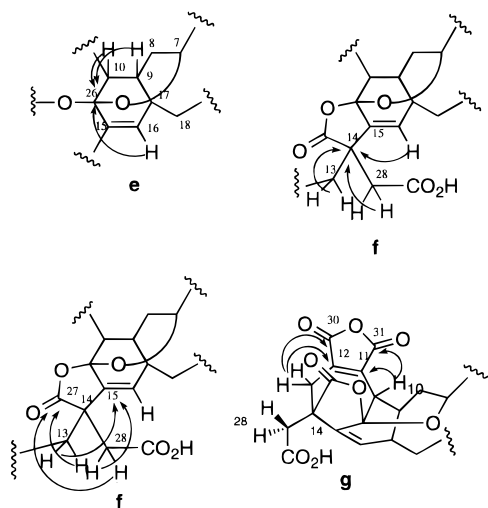
Figure 2. Long-range $^1H-^{13}C$ correlations observed in the HMBC NMR spectrum of **2**.

Figure 3. Structures of **1** and **2**.

Figure 4. Relative stereochemistry of the acetal ring.

Hz) implies *E* configurations in the propenyl groups at the chain ends. The carbon at C-20 was inserted between C-19 and C-21 on the basis of the gradation in carbon T_1 (C-20 has an nT_1 of 0.76 s in compound **1**, with 0.49 s for C-19 and 1.17 s for C-21) when all connections in the cage had been satisfied.

Assembly. The fragments **a**−**d** were deduced using the NMR spectra of both compounds **1** and **2** up to this point. Since the spectra of **2** were in general better resolved, the rest of the assembly was performed mainly on the basis of the spectra of **2**. Starting with the unit $\rangle C_{10}-C_9(R_1)-C_{17}(R_2)-C_{16}=\langle$ already established, the rest of compound **2** was assembled as follows (Figure 2):

1. The lactol carbon at 104.8 ppm (C-26) is correlated with protons H-9, H-10, and H-16, which requires its ends to close a 6-membered ring onto C-15, yielding partial structure **e** (Figure 2). In compound **2**, a second ring is closed via an oxygen link between C-26 and C-7 in the R_1 side chain.

2. Quaternary carbon C-14 (47.3 ppm) shows a crosspeak to the vinyl proton at 5.65 ppm and must therefore be connected to a vinyl carbon in that assembly. C-14 is also coupled to the protons in the two remaining methylene groups with chemical shifts at 3.06, 2.71 ppm and 3.29, 2.95 ppm, respectively, which are not connected to each other. Two carbons (the carbonyl at 175.3 ppm and the vinyl carbon at 139.8 ppm) correlate with (two different sets of) protons on *both* methylene groups, so that the carbon atoms connected to C-14 must be C-27, C-15, C-13, and C-28. A ROESY experiment (see below) was used to determine that the methylene group with protons at 3.29 and 2.95 ppm is exocyclic, and therefore, the carbonyl at 175.3 (C-27) connects to C-26 as shown in **f**. The carboxyl at 173.8 ppm shows an HMBC correlation with both H-28 protons, completing its valence.

3. Vinyl carbons at 141.5 and 140.3 ppm are both coupled to H-10 and H-13, while carbonyl groups at 164.4 and 164.3 ppm couple to only H-10 and H-13 protons, respectively. The net effect is to form a maleic anhydride ring which links units C-10 and C-13, closing another ring in the assemblage (**g**). The high-field shifts of these carbonyls are in agreement with the UV spectrum, which indicated the presence of α,β-unsaturated carbonyls. The weak COSY correlation between H-10 and one of the H-13 protons is attributed to homoallylic coupling.

As mentioned above, vinyl carbon C-15 and carbonyl C-27 each correlate with different protons in both methylene units C-13 and C-28, reflecting the stereospecific nature of vicinal
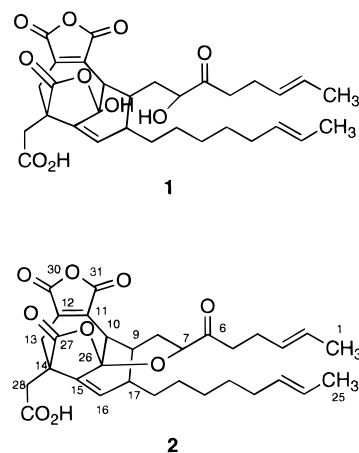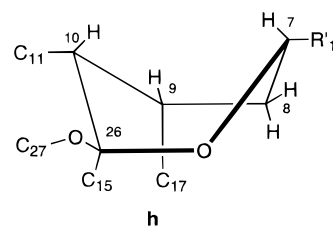
spin coupling. The 5-membered lactone ring closed implicitly in step 2 of the assembly places these carbons in an opposite array with respect to specific methylene protons, provided that the torsion angle about the C-14−C-28 single bond is fixed as shown in **g**. A 300 ms spin-lock ROESY experiment showed selective cross polarization between the vinyl proton and the high-field methylene H-13 and H-28 (i.e., those which show the HMBC correlation with the carbonyl at C-27). This both confirms the architecture shown in **g** and implies that the 70 ms HMBC correlations (optimum $^nJ_{C,H}$ of 7 Hz) to C-8 and C-15 all result from a near anti-periplanar arrangement.

On the basis of the foregoing spectral analysis, the gross structure of compound **2** is established as shown in Figure 3. This also establishes the structure of **1** which is a hemiacetal congener of compound **2**.
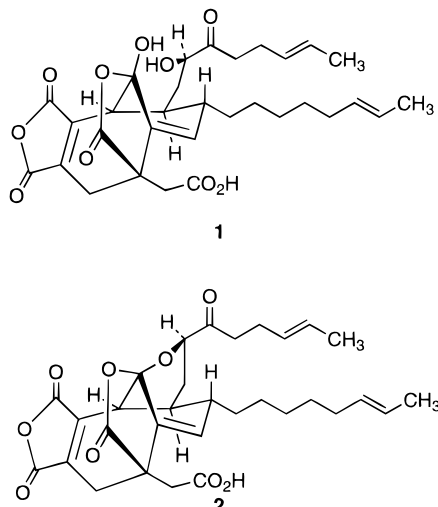
Relative Configurations. The configurations of the C-11, C-12 and C-15,C-16 double bonds and relative configurations about the asymmetric centers at positions C-10, C-14, and C-26 are all fixed by the steric requirements of the cage, leaving only positions C-7, C-9, and C-17 to be specified. Molecular models indicate that the 6-membered ring bearing the two side chains has an approximate boat conformation with prows at positions C-17 and C-26.

C-7 and C-9 are included in the added 6-membered ring in compound **2**, which constrains the relative configuration at position 9 to that shown in Figure 4. H-7 is coupled to the low-field methylene proton H-8a by 7.8 Hz and to H-8b by 9.2 Hz. These values are outside the range of a normal chair conformation in which at least one pair of protons must be *gauche*, forcing one to consider the only possible boat configuration, sketched in **h**, where positions 7 and 10 are at the prows. The coupling constants then become reasonable on the condition that H-7, like H-10, occupies the *endo* position. Both arguments are confirmed by a strong ROESY correlation between H-7 and H-10, which is possible only for a boat configuration such as **h**, fixing the relative configuration at position 7 independently of that at position 17. The presumed reason for a boat conformation in the added ring is to minimize steric crowding between the cage and the remainder of the R_1 side chain.

Table 2. ^{1}H$-^1$H Spin Coupling Constants for **1** and **2**

positions	$^3J_{H,H}$		positions	$^3J_{H,H}$	
	1	**2**		**1**	**2**
16,17	3.3	2.2	9,8b	~0	
9,17	7.6	4	7,8b	7.8	9.2
9,10	u^a	4	7,8a	3.5	7.8
9,8a	7				

^{a} u = not accurately measurable.

Figure 5. Relative stereochemistry of **1** and **2**.

The weak $^3J_{H,H}$ couplings about the C-16,C-17 and C-9, C-10 single bonds imply H,H dihedral angles near 90°. The computed dihedral angle about the C-9,C-10 bond is consistent with the established configuration at C-9, while that about the C-16, C-17 bond (107° vs 15°) favors the configuration at C-17 in which the side chains are *trans*. The $^3J_{H9,H17}$ coupling constant, while substantial, was not accurately measurable and, on the basis of the computed angles (144° vs 32°), would not be definitive at any rate. A significant interaction between the side chains is reflected by the changes of ^{1}H chemical shift and diastereotropy in the first three methylene units of R$_2$ due to the change in R$_1$ between **1** and **2** (Table 2). The stereochemistry at C-17 was established by time-dependent NOE experiments on **1**. The NOE experiments indicated that the distance between H-9 and H-17 is approximately 10% longer than that of H-9 and H-10. Molecular-modeling calculations show that if H-9 and H-17 are *trans* to each other, this interproton distance is longer than the distance between H-9 and H-10, whereas if *cis*, it would be shorter than the distance between H-9 and H-10. On the basis of this finding, the stereochemistry of H-9 and H-17 was determined to be *trans*. From the interconversion experiments cited before it was concluded that the C-9 side chain was on the same face as the C-26 carbon. Therefore, the *trans* relationship of H-9 and H-17 implies that the relative stereochemistry of compound **2** is as shown in Figure 5.

On the basis of the interconversion experiments the structure of compound **1** was subsequently established as shown in Figure 5. The configuration at C-7 is assumed to be the same as in **2** on the basis of the likely mechanism that the C-7 hydroxy group replaces the C-26 hemiacetal hydroxy group. If the acetal formation was achieved by the C-26 hydroxy group replacing the C-7 hydroxy group, the stereochemistry at C-7 would become ambiguous and could not be assigned.

One of the striking features of these compounds is the presence of a bridgehead (anti-Bredt) alkene moiety. It is contained in a bicyclo[4.3.1]deca-1,6-diene system which ac-

cording to the Bredt's rule and its revision[10,11] should be stable at room temperature. Indeed, the parent system, bicyclo[4.3.1]-deca-1-en-10-one, has been synthesized and shown to be stable at room temperature.[12] Compounds **1** and **2** thus constitute a small group of natural products possessing a bridgehead double bond,[13] which includes the taxanes with a bicyclo[5.3.1]undeca-1-ene system.[14] The other prominent feature of the new compounds is a cage-like core structure which is constructed partially by the γ-lactol or γ-lactol acetal moiety. These are formed presumably due to the entropic factor of interacting groups in close proximity.

It is proposed that these compounds are related to nonadrides since they can be conceptually dissected to a compound containing a 9-membered ring (see structure *i*, Figure 6) to which a maleic anhydride moiety is annealed. The nonadrides include glaucanic acid,[15] glauconic acid,[15] byssochlamic acid,[16] scytalidic acid,[17] heveadride,[18] casteneinolide,[19] and rubratoxins A and B.[20,21] On the basis of the published work on the biosynthesis of glauconic acid[22] and a proposed biosynthesis of rubratoxins,[23] the biosynthetic pathway of **1** and **2** can be rationalized as shown in Figure 6. Thus, they can arise from a head-to-head condensation of two 16-carbon units which in turn are formed from lauric acid (or another 12-carbon acid) and oxaloacetic acid. For example, the 16-carbon unit, decylcitric acid, is a known fungal metabolite.[24] A loss of one carbon unit for glauconic acid by decarboxylation from the top half of structure *i* in Figure 6 would give the total carbon count of 31, as in **1**. As mentioned earlier, this producing organism yields zaragozic acid A in addition to compounds **1** and **2**. Recently, citric acid derivatives with a long *ara*-alkyl chain corresponding to the zaragozic acid A or B backbone (L-731,120 and L-731,128) have been reported as minor components of zaragozic acid A or B fermentation broths.[25] These citric acid derivatives can be rationalized as the products of oxaloacetic acid condensation with the corresponding 19- and 21-carbon monocarboxylic acids.[26] Therefore, it can be further hypothesized that the condensation of oxaloacetic acid with the respective monocarboxylic acid is a common biosynthetic

(10) Buchanan, G. L. *Chem. Soc. Rev.* **1974**, *3*, 41−63.
(11) Köbrich, G. *Angew. Chem., Int. Ed. Engl.* **1973**, *12*, 464−473.
(12) Cordiner, B. G.; Vegar, M. R.; Wells, R. J. *Tetrahedron Lett.* **1970**, 2285−2286.
(13) Yamamura, S. *Kagaku Seibutsu* **1976**, *14*, 391−393.
(14) Nicolaou, K. C.; Dai, W.-M.; Guy, R. K. *Angew. Chem., Int. Ed. Engl.* **1994**, *33*, 15−44.
(15) Barton, D. H. R.; Sutherland, J. K. *J. Chem. Soc.* **1965**, 1769−1972.
(16) Baldwin, J. E.; Barton, D. H. R.; Sutherland, J. K. *J. Chem. Soc.* **1965**, 1787−1798.
(17) Strunz, G. M.; Kakushima, M.; Stillwell, M. A. *J. Chem. Soc., Perkin Trans.* **1972**, *1*, 2280−2283.
(18) Crane, R. I.; Hedden, P.; MacMillan, J.; Turner, W. B. *J. Chem. Soc., Perkin Trans.* **1973**, *1*, 194−200.
(19) Arai, K.; Shimizu, S.; Miyajima, H.; Yamamoto, Y. *Chem. Pharm. Bull.* **1989**, *37*, 2870−2872.
(20) Buchi, G.; Snader, K. M.; White, J. D.; Gougoutas, J. Z.; Singh, S. *J. Am. Chem. Soc.* **1972**, *92*, 6638−6641.
(21) Moss, M. O.; Robinson, F. V.; Wood, A. B. *J. Chem. Soc. C* **1971**, 619−624.
(22) Bloomer, J. L.; Moppett, C. E.; Sutherland, J. K. *J. Chem. Soc. C.* **1968**, 588−591.
(23) Moss, M. O. In *Microbial Toxins*; Ciegler, A., Ed.; Academic Press: New York & London, 1971; Vol. 6, pp 381−407.
(24) Gatenbeck, S.; Måhlén, A. *Acta Chem. Scand.* **1968**, *22*, 2613−2616.
(25) Huang, L.; Lingham, R. B.; Harris, G. H.; Singh, S. B.; Dufresne, C.; Nallin-Omstead, M.; Bills, G. F.; Mojena, M.; Sanchez, M.; Karkas, J. D.; Gibbs, J. B.; Clapp, W. H.; Meinz, M. S.; Silverman, K. C.; Bergman, J. D. *Can. J. Bot.* **1995**, *73*, S898−S908.
(26) Bergstrom, J. D.; Dufresne, C.; Bills, G. F.; Nallin-Omstead, M.; Byrne, K. *Annu. Rev. Microbiol.* **1995**, *49*, 607−639.
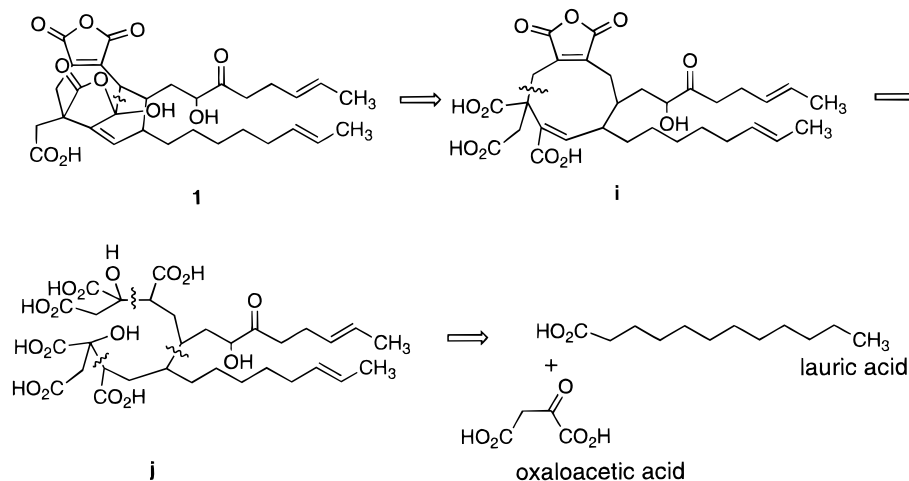
Figure 6. Potential biosynthetic units of **1**.

pathway for both nonadrides[27] and zaragozic acids. Because of the condensed ring systems and oxidative modifications of the side chains, compounds **1** and **2** appear to be one of the most complex nonadrides isolated to date.

Experimental Section

Instrumentation. ^{1}H and ^{13}C spectra NMR were recorded on a Bruker AM500 at 500.13 and 125.75 MHz, respectively. IR spectra in KBr were measured on a Nicolet 510 FT-IR spectrometer. FAB-MS spectra were obtained on a Kratos Concept mass spectrometer using a matrix of thioglycerol containing sodium iodide. HR FAB-MS spectra were obtained on a VG Analytical ZAB-2SE double-focusing mass spectrometer using a matrix of *m*-nitrobenzyl alcohol and PEG 400. Optical rotations were measured on a Perkin-Elmer 241 MC polarimeter.

NMR experiments were typically performed using approximately a 200 ppm carbon spectral width and an 8 ppm proton spectral width. Relaxation delays were generally 1.0 s, and data were acquired at ambient temperature. Chloroform was used as both proton (7.27 ppm) and carbon (77.0 ppm) chemical shift reference. Waltz decoupling was employed for proton decoupling, and GARP decoupling was used for carbon decoupling. 2D NMR experiments were conducted using standard pulse sequences and methods. COSY experiments were performed by acquiring 1024×256 data points, and the data were processed with unshifted sine bell weighting to 1024×1024 by zero-filling twice. Long-range COSY experiments were performed in an identical manner using an 80 ms contact time. HETCOR experiments were performed by acquiring 8192 points in the direct (carbon) dimension and 224 points in the indirect dimension. The data were processed to 8192×512 using a 90° sine bell squared weighting. The spectral widths were 25 000 Hz for ^{13}C and 1225 Hz for [1]H. HMBC experiments were performed in inverse-detection mode using a 62 ms

contact time by acquiring 4096×512 points and processing to 4096×2048 using a 90° sine bell squared weighting. Data were acquired pure-phase using TPPI. The 300 ms ROESY data were collected as 2048×300 points, weighted using a 90° squared sine bell, and zero-filled to 2048×1024 points. States−TPPI was used to obtain pure-phase data. Time-dependent nuclear Overhauser effect (NOE) experiments were performed on a Bruker DMX-500 NMR spectrometer operating at 500.13 MHz. Data were acquired with interleaved on-resonance/off-resonance irradiation and 128 scans total for each time point. The NOE was measured at 50, 100, 150, 300, 400, 500, and 800 ms and 1.2 and 2 s, and quantitated by comparing the integral under the direct peak (H-9) to the integrals of the NOE peaks. The initial rates were measured by approximating the early part of the time course with a straight line (significant deviation from linearity begins at approximately 400 ms).

Conversion of 1 to 2. CP-225,917 (**1**, 1 mg, 1.8 μmol) was dissolved in 2 mL of anhydrous dichloromethane. To this solution was added 1.8 μL of methanesulfonic acid (0.1 M in dichloromethane), and the resulting solution was stirred at room temperature. At the appropriate time point, an aliquot was withdrawn and injected into an HPLC (Microsorb C_{18} column, 0.1% H_3PO_4/CH_3CN = 3:7). Compound **1** (retention time 5.95 min) was gradually converted to compound **2** (retention time 10.08 min), and the conversion was complete within 24 h at room temperature.[28] A parallel experiment starting with compound **2** in water-saturated dichloromethane containing a catalytic amount of methanesulfonic acid did not show any change after 24 h.

(27) Turner, W. B. In *Fungal Metabolites*; Academic Press: New York, 1971; pp 292−294.

(28) When the reaction was carried out at 75 °C in dichloroethane, the conversion of **1** to **2** was complete within 6 h and a third peak (retention time 10.6 min) subsequently appeared, whose structure has not been determined.